MIT Libraries | DSpace@MIT

MIT Open Access Articles

Positron annihilation lifetime spectroscopy: When is it feasible to decompose the spectrum?

The MIT Faculty has made this article openly available. ***Please share*** how this access benefits you. Your story matters.

Citation: Logan, JV, McAlpine, SW, Webster, PT, Morath, CP and Short, MP. 2021. "Positron annihilation lifetime spectroscopy: When is it feasible to decompose the spectrum?." Journal of Applied Physics, 130 (14).

As Published: 10.1063/5.0049304

Publisher: AIP Publishing

Persistent URL: https://hdl.handle.net/1721.1/147620

Version: Author's final manuscript: final author's manuscript post peer review, without publisher's formatting or copy editing

Terms of use: Creative Commons Attribution-Noncommercial-Share Alike

Massachusetts Institute of Technology

ACCEPTED MANUSCRIPT
Journal of Applied Physics
AIP Publishing
This is the author's peer reviewed, accepted manuscript. However, the online version of record will be different from this version once it has been copyedited and typeset.
PLEASE CITE THIS ARTICLE AS DOI: 10.1063/5.0049304

Positron Annihilation Lifetime Spectroscopy: When is it feasible to decompose the spectrum?

J. V. Logan,[1, 2, a)] S. W. McAlpine,[1] P. T. Webster,[2] C. P. Morath,[2] and M. P. Short[1]
[1)]*Department of Nuclear Science and Engineering, Massachusetts Institute of Technology, 77 Massachusetts Ave, Cambridge, MA 02139 USA*
[2)]*Air Force Research Laboratory, Space Vehicles Directorate, Kirtland AFB, NM 87117 USA*

(Dated: 21 September 2021)

Positron annihilation lifetime spectroscopy (PALS) has the potential to determine open volume defect identities and concentrations, only if the spectrum can be accurately decomposed into its constituent parts. The intrinsic difficulty of decomposing PALS spectra into their constituent lifetimes and intensities is demonstrated, and it is shown that the global minimum of the objective function does not represent the true solution for a range of typical experimental scenarios. We show that the function currently employed in standard fitting methods cannot be improved upon with alternate weighting schemes. Resolution function width minimally impacts fit decomposition quality, but errors are reduced with higher counts. A regression model is developed based on the experimental count, intensity of the defect component, and difference between the defect and bulk lifetime which predicts the anticipated intrinsic error of the objective function global minimum in estimating the fraction of positrons which annihilate in the bulk. This can be employed to determine whether a given PALS spectrum can be successfully decomposed into defect types and lifetimes.

I. INTRODUCTION

Positron annihilation lifetime spectroscopy (PALS) is a powerful material characterization technique that can be used to characterize concentrations and types of open volume defects in materials. When positrons enter perfect crystals, they will thermalize, diffuse, and eventually annihilate with a bulk lifetime characteristic of the material. If the material contains open volume defects, whether by design, by off-stoichiometry, or due to radiation damage, the positron may become trapped by their attractive potential and annihilate, with a lifetime characteristic to the defect. The positron lifetime is a function of the electron density at the annihilation site, with lower electron density associated with longer positron lifetimes. The fraction of positrons annihilating with different lifetimes can allow one to experimentally assess open volume defect concentrations and types. This attribution is predicated on the ability to decompose the experimental spectrum to obtain the lifetimes and intensities. This decomposition is an inherently ill-conditioned problem due to incompleteness in the data and noise.[1,2]

The difficulty of achieving a consistent decomposition is illustrated in a literature review of recent PALS studies.[3] The deviation between groups of the values reported for the bulk lifetime is significantly larger than statistical errors reported. For example, considering five recent studies, the standard deviation for the fit bulk lifetime in GaAs is 5.043 ps and for ZnO is 6.618 ps.[3] The deviation in defect lifetimes is even larger. This inconsistency can lead to significant errors in reported defect types and concentrations.[3] Many studies present only the average lifetime or the average lifetime alongside the decomposition while questioning the validity of the presented 2-component decomposition.[4–11] This is done because the average lifetime is statistically accurate even if an incorrect lifetime decomposition is obtained. However, the average lifetime value inherently contains less information than would a decomposition.[2,3]

The experimentally obtained PALS spectrum $N(t)$ is the probability of a positron to annihilate at time t (time derivative of the probability that a positron exists at time t), which is a summation over annihilation in the bulk and in d defect types ($d+1$ components). In a theoretical experiment with no uncertainty, this spectrum represents the total count of positrons annihilating at time t

$$N_{theo}(t) = \sum_{i=1}^{d+1} I_i \lambda_i e^{-\lambda_i (t-T_0)} \tag{1}$$

in which $\lambda_i = 1/\tau_i$ is the characteristic annihilation rate (inverse lifetime) and $I_i(t)$ is the normalized intensity of the i^{th} annihilation component. T_0 is an offset in time caused by signal propagation delay in experiment cables. Experimental spectra will also be convolved with an instrument resolution function (IRF) due to uncertainties in the acquisition system, which is often taken to be the weighted sum of g Gaussian functions which are permitted to be shifted with respect to each other.[12] The resulting convolution has an analytical form, given by

$$N(t) = \frac{1}{2} \sum_{i=1}^{d+1} I_i \lambda_i \sum_{j=1}^{g} w_j e^{-\lambda_i u_j + \frac{1}{2}\lambda_i^2 \sigma_j^2} \operatorname{erfc}\left(\frac{\lambda_i \sigma_j^2 - u_j}{\sqrt{2}\sigma_j} \right) \tag{2}$$

in which erfc() is the complementary error function, $u_j = (t - T_0 - \Delta_j)$, and σ_j, Δ_j, and w_j are the standard deviation, shift, and weight of each Gaussian component.[12] The lifetime intensities and Gaussian weights are normalized, so each of the fit parameter numbers can be reduced by one given that $I_{d+1} = 1.0 - \sum_{i=1}^{d} I_i$ and $w_g = 1.0 - \sum_{i=j}^{g-1} w_j$. Spectra will conventionally be composed of bulk annihilation, a given number of defect lifetime(s), one lifetime for surface

[a)]Electronic mail: jvl2xv@mit.edu.

Approved for public release; distribution is unlimited. Public Affairs release approval AFRL-2021-0604.

ACCEPTED MANUSCRIPT
Journal of Applied Physics
AIP Publishing
This is the author's peer reviewed, accepted manuscript. However, the online version of record will be different from this version once it has been copyedited and typeset.
PLEASE CITE THIS ARTICLE AS DOI: 10.1063/5.0049304

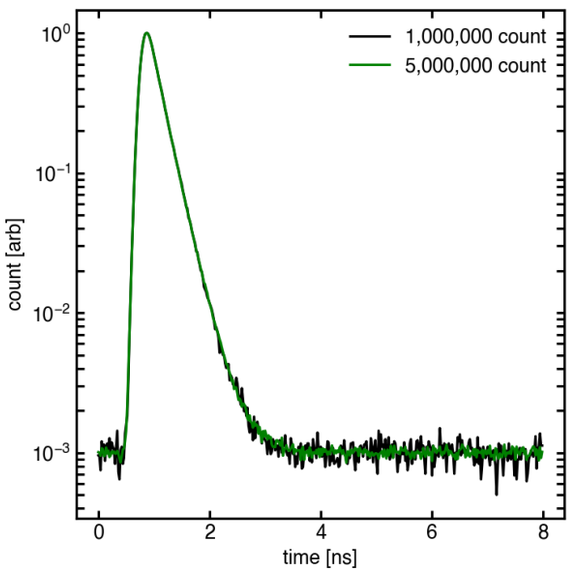

FIG. 1. Representative, simulated, ideal PALS spectrum for monocrystalline Si. This spectrum represents 35% annihilation in bulk with τ_B = 0.22 ns, 60% in monovacancies with τ_2 = 0.25 ns, and 5% in salt with τ_3 = 0.37 ns. The IRF has two components and a FWHM of 0.19 ns (Table I). The spectra are simulated with representative Poisson noise, shown for realistic annihilation counts of 1,000,000 and 5,000,000. These are generated employing Eq. 2 and Poisson sampling.

TABLE I. Parameters of the IRF assumed in this analysis. These parameters are representative of those which can be obtained experimentally. The fit extends to 8.0 ns with 0.02 ns bins, the background fraction is 0.001, and the T_0 is equal to 0.8 ns. Fitting begins to the left of the maximum at the bin associated with half the maximum.

Parameter	Gaussian 1	Gaussian 2
FWHM [ns]	0.18	0.18
Shift Δ [ns]	-0.05	0.0
Weight w [frac]	0.5	0.5

positronium[2], and an annihilation component associated with the positron source itself (annihilation in source ^{22}NaCl salt and any foils used for source encapsulation). Although, it should be noted that use of a slow positron beam or direct ^{22}NaCl deposition on the sample surface can remove some of these additional terms. Illustrative, idealized PALS spectra for monocrystalline Si are given in Fig. 1, assuming 35% annihilation in bulk with τ_B = 0.22 ns[13–15], 60% in monovacancies with τ_2 = 0.25 ns, and 5% in salt with τ_3 = 0.37 ns; a 2-component IRF of full-width-at-half-maximum (FWHM) of 0.19 ns; and Poisson noise associated with experimental counts of 1,000,000 and 5,000,000. These are generated employing Eq. 2 and Poisson sampling. The resolution function parameters and other relevant spectral properties are summarized in Table I. This simple yet representative spectrum and IRF are used throughout this analysis as the base fitting case.

The experimental spectrum is typically fit to the function defined in Eq. 2 with the fitting parameters being positron lifetimes, intensities, and Gaussian parameters (standard deviations, shifts, and weights). Due to the large number of parameters to be fit, the IRF parameters are typically obtained in preliminary fits,[12] reducing the number of fit parameters to just the intensity and lifetime of the bulk and each defect present in the material. The bulk lifetime of most common materials has been determined experimentally and through simulation in literature, as have some characteristic defect lifetimes, although there exists substantial uncertainty.[2,3] This uncertainty stems mostly from the difficulty of the fitting problem.[2]

The bulk lifetime is related to other parameters through[2]

$$\tau_B = \left(\sum_{i=1}^{d+1} \frac{I_i}{\tau_i} \right)^{-1} \tag{3}$$

As such, confident knowledge of the bulk lifetime can permit reduction in the number of lifetimes fit by one (or this relation can be used to check the potential validity of a decomposition). In the PALS spectrum, the defect lifetimes measured will be equal to their characteristic values, but the first 'bulk' lifetime value will vary based on defect identities and concentrations. For this reason, the first bulk lifetime value should be the one which is solved for if the defect identities are known and their lifetimes can be fixed to known values.

A commonly employed fitting software is PALSFIT3, which uses an iterative, separable, least-squares fitting method to fit the spectrum in which some parameters enter nonlinearly.[2] As an objective function to be minimized, this software employs a statistically weighted least-squares criterion

$$\Phi = \sum_{k=1}^{n} w_k (y_k - f_k(b_1, ..., b_m))^2 \tag{4}$$

in which n is the number of data in the spectrum, y_k is the measured spectral value in time bin k, w_k is the weight applied to the error in count in bin k, and $f_k(b_1, ..., b_m)$ is the evaluation of Eq. 2 at time bin k given fit parameters $b_1, ..., b_m$. PALSFIT3 employs a statistical weighting in which the weight is the inverse variance of the counts. Due to the fact that this is a Poisson random process, $w_k = \frac{1}{\sigma_k^2} = \frac{1}{y_k}$.[12]

For the spectrum visualized in Fig. 1 (5,000,000 counts) and using the objective function in Eq. 4, one can sample the potential parameter space for this spectrum and obtain the multi-dimensional objective function surface. This is significant because the existence of a clear global minimum which represents the true solution would imply that fitting algorithms should be able to obtain the correct solution. Assuming perfect knowledge of the IRF and sampling the space of potential 3-lifetime value and intensity combinations (with τ_1 solved for using Eq. 3 and knowledge of τ_B of Si, and I_1 found through normalization) surrounding and including the true parameters for the Fig. 1 spectrum, the objective function space is plotted in Fig. 2 projected onto the I_1 axis. The point associated with the parameter combination which yields the minimum objective function is shown in red (cross) and the points associated with the next four minimal objective function parameter combinations are shown in blue (circles). The vertical

Approved for public release; distribution is unlimited. Public Affairs release approval AFRL-2021-0604.

ACCEPTED MANUSCRIPT
Journal of Applied Physics
AIP Publishing
This is the author's peer reviewed, accepted manuscript. However, the online version of record will be different from this version once it has been copyedited and typeset.
PLEASE CITE THIS ARTICLE AS DOI: 10.1063/5.0049304

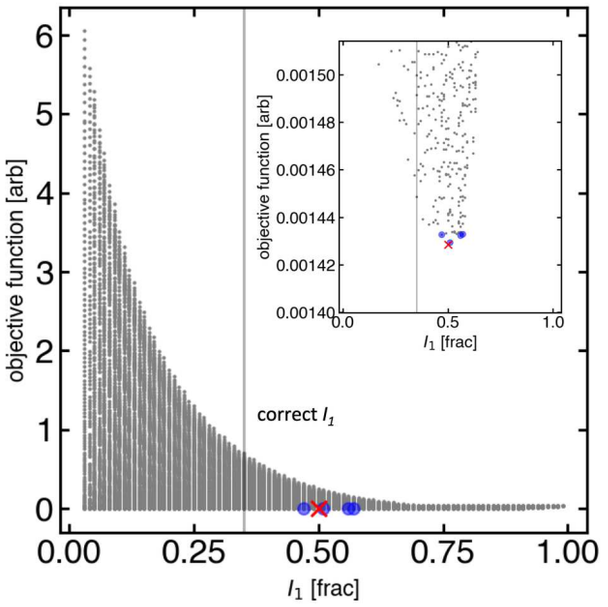

FIG. 2. Objective function surface projected onto the I_1 parameter for the 5,000,000 count spectrum visualized in Fig. 1 assuming perfect knowledge of the IRF (Table I) and sampling the entire parameter space surrounding and including the true solution. The point associated with the parameter combination which yields the minimum objective function (global minimum) is shown as a red cross, and the points associated with the next four minimal objective function parameter combinations are shown as blue circles. The vertical line represents the correct $I_1 = 35\%$. The inset shows a magnification near the minimal objective function values.

line represents the correct $I_1 = 35\%$. It is clear that the global minimum of the objective function yields an incorrect solution. It should be recalled that this inability to identify the global minimum occurs in a semi-ideal case in which we have perfect knowledge of the IRF and large defect intensity.

Frequently in literature, if the authors are unable to obtain realistic fits with physical meaning, only the average positron lifetime (center of mass of the lifetime spectrum) given by

$$\tau_{avg} = \sum_{i=1}^{d+1} I_i \tau_i \tag{5}$$

is reported. This value can be calculated with high reliability and allows defect concentration trends to be confidently reported, theoretically independent of the accuracy of the particular defect decomposition. Average lifetime differences of less than 1 ps can be consistently observed experimentally, resulting in a precise, repeatable measurements.[2,16] For example, the average lifetime for the spectrum visualized in Fig. 1 is 0.231 ns (again an idealized case), which differs substantially from the experimentally known, bulk lifetime in Si of 0.220 ns.

In this study, we improve upon standard PALS spectral decomposition methods by performing the following: (1) analyze the optimality of the most commonly employed objective function (Eq. 4); (2) assess the impact on fitting accuracy caused by different experimental design considerations; and, (3) provide a criterion to predict whether for a given physical scenario one should anticipate that an accurate lifetime decomposition can be obtained, or whether τ_{avg} in Eq. 5 should be reported instead.

II. RESULTS

A. Objective Function Optimality

In this section, we assess the optimality of the objective function employed by the most commonly used fitting software, given in Eq. 4, and consider others[12]. In doing so, we assume the most ideal case in which the IRF is known with perfect accuracy (the parameters of which are given in Table I). Six different weighting schemes are considered: (1) division by counts $[1/c]$, (2) division by counts squared $[1/c^2]$, (3) division by the square root of the counts $[1/\sqrt{c}]$, (4) multiplication by the square root of the counts $[\sqrt{c}]$, (5) multiplication by the counts $[c]$, and (6) unweighted. Unweighted fitting routines inherently prioritize high intensity data (and therefore shorter lifetimes in PALS) in the decay, as the least-squares residual will be most effectively minimized by reducing error in the high intensity side of the curve at the expense of poor fit quality several orders of magnitude down in the low intensity, long positron lifetime regime. On the other hand, weighting the data with counts in the denominator serves to "normalize" the least-squares minimization, so that a percentage error on the high intensity side is weighted identically to the same percentage error on the low intensity side. The result is that fits weighted by $1/c$ are more capable of characterizing features in positron lifetime data spanning several orders of magnitude, as is the case here where low intensity, long lifetime signals from defects may only be resolvable after the high intensity, short lifetime signal from the bulk has substantially decayed. Using the experimental spectrum visualized in Fig. 1 with 50 different variants based on repeated Poisson noise sampling and resolution summarized in Table I, each objective function is judged in terms of the absolute value of the error in I_1 of its global minimum. The error bars in Fig. 3 show the standard deviation of the 50 samples for each objective function. From this figure, one cannot statistically distinguish the objective functions, but the traditionally employed division by experimental count provides the minimum average error and is used in the remainder of this analysis.

The meaning of this division by counts weighting is visualized in Fig. 4. This figure shows the raw objective function values for the true solution (red) and negative of the raw objective function values for the global minimum of the objective function (blue) as a function of spectral time bin. The cumulative difference between these two is shown in black and the spectrum itself (without noise) is superimposed for comparison in gray. It is shown that the contributions to the objective function are of the same order of magnitude over the entire fit range, but that the global minimum makes itself superior in the region where the spectrum is less than one quarter of its

Approved for public release; distribution is unlimited. Public Affairs release approval AFRL-2021-0604.

ACCEPTED MANUSCRIPT
Journal of Applied Physics
AIP Publishing
This is the author's peer reviewed, accepted manuscript. However, the online version of record will be different from this version once it has been copyedited and typeset.
PLEASE CITE THIS ARTICLE AS DOI: 10.1063/5.0049304

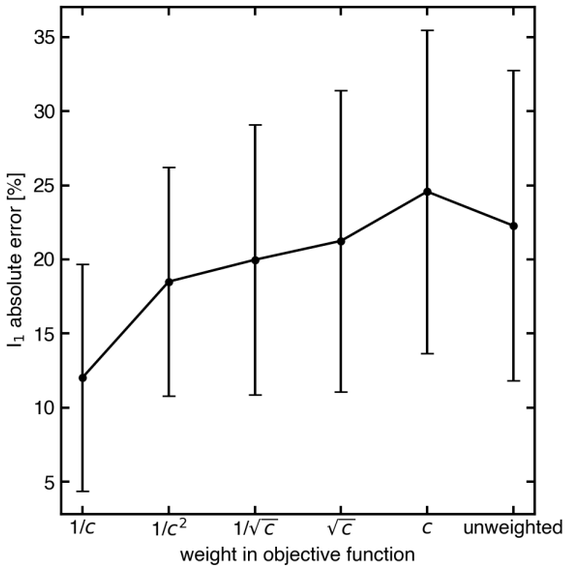

FIG. 3. For 50 Poisson noise variants of the 5,000,000 count spectrum visualized in Fig. 1 (IRF summarized in Table I), the average absolute error of the global minimum of the objective function in the first bulk lifetime intensity I_1. The error bars show the standard deviation over the 50 Poisson spectrum distributions. This is shown as a function of the weighting used in the objective function with c being the experimental count in each time bin.

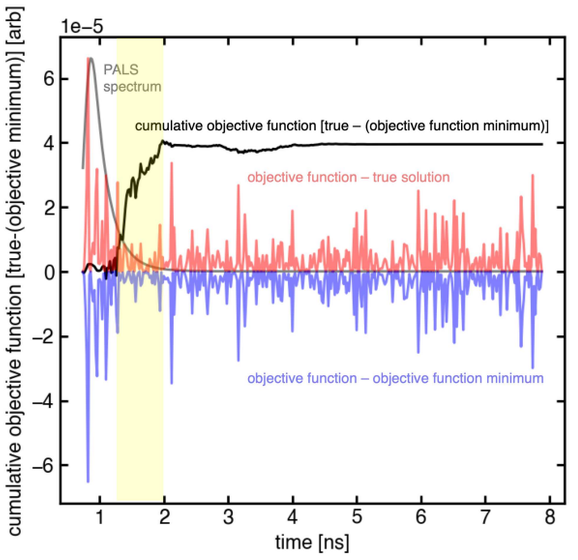

FIG. 4. The cumulative objective function difference for the true spectrum and the minimum of the objective function (black) as a function of spectral time [ns] for a 5,000,000 count spectrum visualized in Fig. 1 (IRF summarized in Table I). The individual objective functions for the true and global minimum solutions are visualized in red and blue respectively as a function of spectral time [ns] and the spectrum itself (without noise) is visualized in gray. The time scales over which the objective function minimum distinguishes itself from the true solution are highlighted in yellow.

maximum value (where longer lifetimes dominate) as shown in the yellow shaded region of Fig. 4. The reason why long-time objective function maxima have no impact on the cumulative objective function difference is because both the true and global minimum spectra fail to capture this noise in the spectrum to the same degree. In contrast for an unweighted objective function or an objective function weighted by count, the dominant contributions to the difference in the objective function occur at shorter time scales, however, this approach is shown in Fig. 3 not to improve accuracy of the objective function in indicating the true lifetime decomposition.

B. Experimental Parameter Optimization

There exist many experimental and fitting parameters that can have impact on the ability of the objective function to appropriately indicate the true solution. These include: (1) the experimental count; (2) the IRF width; (3) the error in the IRF estimation; (4) the time-bin width in the acquired spectrum (for equivalent total count); (5) the time bin at which fitting begins; (6) the time bin at which fitting ends; and, (7) smoothing of experimental data. When not otherwise specified, values indicated in Table I and Fig. 1 are used throughout this optimization.

The dependence of the absolute value of the error of the first lifetime (bulk) intensity [%] of the global minimum objective function on the experimental count is visualized in Fig. 5. It is observed that for unrealistic counts on the order of 100,000,000 the error and statistical spread in the fit errors approaches zero due to the excellent statistics. Acquiring feasible counts of 10^7 rather than 1-2$\times10^6$, is shown to result in lower mean error and smaller statistical variability, underscoring the need to acquire more data than is sometimes published.[17–22]

The IRF width is found to have negligible impact on the ability of the objective function global minimum to be representative of the true solution (Appendix Fig. 8). This does not necessarily indicate that IRF width is unimportant, because it may be easier experimentally to estimate IRF parameters if the overall IRF FWHM is smaller. These findings agree with previous literature in which higher counts are recommended at the expense of IRF width.[23] Errors in IRF width estimation are found to significantly impact the ability to fit (Appendix Fig. 9), with overestimation leading to more severe errors than underestimation. If the IRF width is underestimated (overestimated), the intensity of the bulk lifetime component is underestimated (overestimated) because a larger (smaller) contribution of the larger defect lifetimes is required to compensate for the underestimation (overestimation).

For the experimental time bin width (for equivalent total 5,000,000 counts), it is generally preferred to have larger time bins due to less statistical variability per bin associated with the larger counts per bin, but this effect saturates at time bins of ∼0.06 ns because the spectrum starts to be undersampled and trends start to be missed (Fig. 10). For the bounds of

Approved for public release; distribution is unlimited. Public Affairs release approval AFRL-2021-0604.

ACCEPTED MANUSCRIPT
Journal of Applied Physics
AIP Publishing
This is the author's peer reviewed, accepted manuscript. However, the online version of record will be different from this version once it has been copyedited and typeset.
PLEASE CITE THIS ARTICLE AS DOI: 10.1063/5.0049304

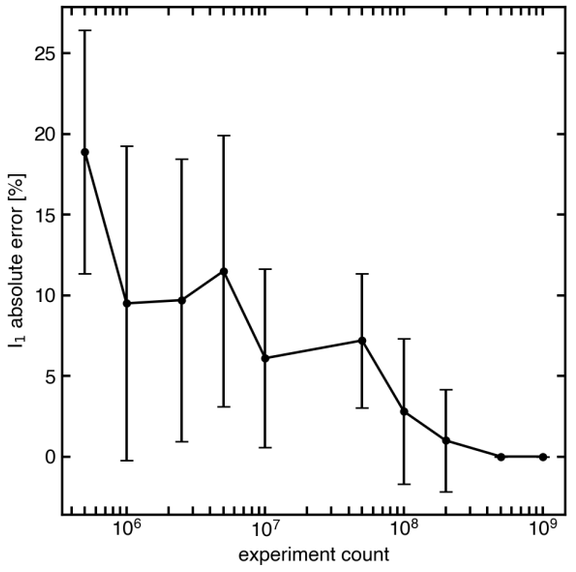

FIG. 5. Dependence of absolute value of the error of the first lifetime (bulk) intensity [%] of the global minimum objective function on the experimental count. The error bars show the standard deviation under 10 Poisson samples of the true function. All unspecified spectral parameters are given in Fig. 1 and Table I.

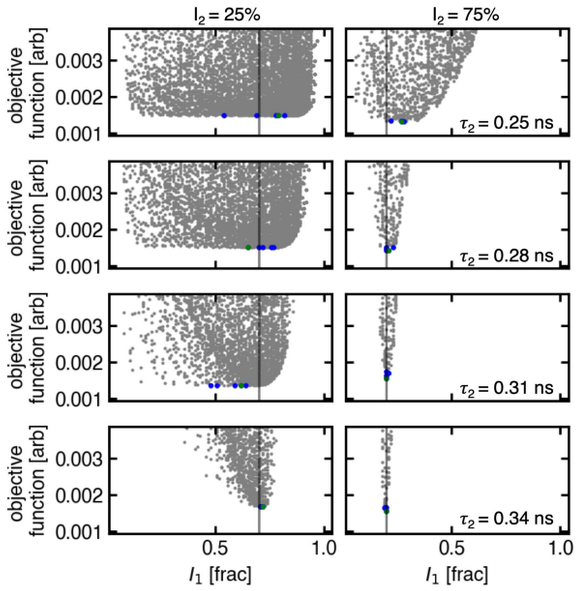

FIG. 6. Objective function surface projected onto the I_1 parameter for an altered 5,000,000 count spectrum visualized in Fig. 1 (different defect intensities in columns and different defect lifetimes in rows) assuming perfect knowledge of the IRF (Table I) and sampling the entire parameter space surrounding and including the true solution. The point associated with the parameter combination which yields the minimum objective function (global minimum) is shown in green and the points associated with the next four minimal objective function parameter combinations are shown in blue (in some cases, two are overlapping). The vertical line represents the correct I_1 (70% column 1, 20% column 1). The defect lifetime increases with rows varying from 0.25 ns to 0.34 ns.

the fit, minimal impact is realized unless the fit start (Appendix Fig. 11) or fit end (Appendix Fig. 12) approach spectral time bins where significant lifetime trends are present. No detriment is observed to fitting out to long time scales on the order of 100 ns. This makes sense with reference to Fig. 3 where it is shown that long-time-scale objective function values do not differentiate the true solution from the global minimum because both fits will have the same errors at these long time scales driven only by experimental statistical variability. Smoothing of the experimental data is found to not improve the ability of the objective function global minimum to approximate the true solution (Appendix Fig. 13).

C. Criterion for Fit Potential

Under optimal fitting, there are still experimental conditions in which the objective function global minimum does not accurately predict the correct lifetime decomposition (Fig. 2). In this section, we develop a criterion which can be used to predict whether under optimal conditions, a reliable decomposition could be obtained (in which the global minimum is clearly representative of the true solution). In general, this condition is met when the defect lifetime(s) present are of large magnitude and have lifetimes which are clearly separated from the bulk lifetime. This trend is visualized in Fig. 6. Each row represents increasing defect lifetime (above the 0.22 ns bulk lifetime of Si) and the first column is for 25% and the second for 75% annihilation in the defect. It is observed that generally for a defect intensity of 25%, a defect lifetime of over 0.34 ns is required to obtain a consistent global minimum (more than the divacancy lifetime in Si). In comparison, for defect concentration of 75%, defect lifetimes of 0.28 ns are sufficient. These effects are studied systematically in this section to provide a criterion to be used to determine if a consistent fit can realistically be obtained.

A regression model is developed to predict mean error of the global minima in predicting the intensity of the bulk lifetime component I_1. In developing the dataset for the model, bulk lifetimes of 0.18 ns to 0.24 ns, counts of 1,000,000 to 50,000,000, differences between bulk and defect lifetimes (τ_2-τ_B) of 0.02 to 0.1 ns, and defect intensities I_2 of 10% to 90% are sampled. The IRF is assumed to be perfectly known (parameters in Table I). The objective function surface is obtained for each parameter combination for 50 Poisson variants of the resulting distribution. The global minimum is identified for each and the average error for the 50 variants is used for model building. This dataset is shown in Fig. 7. It is shown that (τ_2-τ_B) and I_2 are strong predictors of the ability to accurately decompose the lifetime spectrum. The spread in this data results mainly from statistical variability as well as different number of counts in the spectra analyzed.

Through regression, the bulk lifetime is not found to be

Approved for public release; distribution is unlimited. Public Affairs release approval AFRL-2021-0604.

ACCEPTED MANUSCRIPT
Journal of Applied Physics
AIP Publishing
This is the author's peer reviewed, accepted manuscript. However, the online version of record will be different from this version once it has been copyedited and typeset.
PLEASE CITE THIS ARTICLE AS DOI: 10.1063/5.0049304

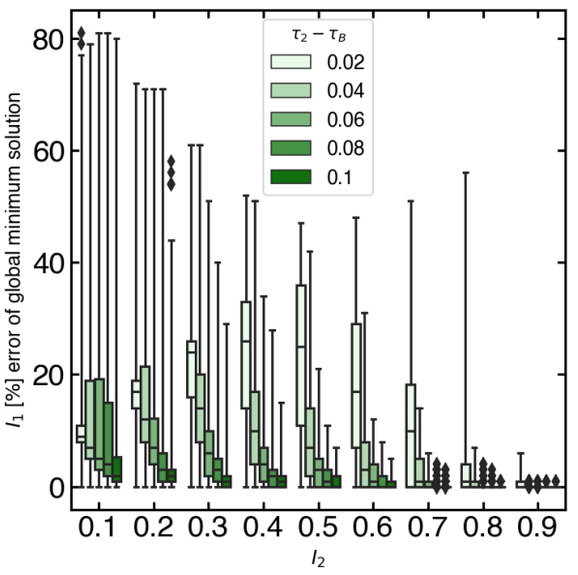

FIG. 7. Data used to develop regression model for predicting error in estimation of the first lifetime component intensity I_1 [%]. The boxplots represent the interquartile range (25%-75%) with the median shown. The x-axis represents the defect intensity and the individual boxplots for each represent increasing difference between the defect and bulk lifetime. Spread in the data represents statistical variability, variability due to different number of counts in the distribution, and any differences due to different bulk lifetime. The whiskers are allowed to extend $22x$ the interquartile range to make obvious the trends of reduced width with increased I_2 and difference between bulk and defect lifetime (points outside this range are defined as outliers and are plotted as diamonds.)

a statistically significant predictor, but counts, (τ_2-τ_B), and I_2 are found to be statistically significant predictors with p-values of less than 0.001. This p-value less than 0.01 indicates that there is sufficient evidence to reject the null hypothesis and conclude that variability in these independent variables is correlated with changes in the dependent variable at the population level. Models with normalized and non-normalized parameters are considered, and the two are found to have identical R^2 statistic (0.740), indicating approximately equal predictive goodness. The non-normalised parameters are presented in Eq. 6 for ease of experimental use (raw experimental parameters can be directly used). All lifetime values should be given in ns, I_2 should be given as a fractional value, and counts should be given as raw counts in the spectrum. The predicted absolute error in I_1 (%) for the global minimum is given by

$$E(I_1) = 28.0 - 165.1(\tau_2 - \tau_B) - 19.2I_2 - \frac{Counts}{1.2 \times 10^7} \quad (6)$$

In this formula, the coefficients of counts, (τ_2-τ_B), and I_2 are all negative because increasing each of these values results in improved ability to decompose the spectrum correctly into its lifetime components. Application of this formula permits experimentalists to predict if there is any potential to accurately decompose their spectra, although accuracy is not ensured because errors in the resolution function estimation may obscure the proper decomposition. Eq. 6 should primarily be used within the range of the data used to generate the model, otherwise extrapolation error will result. Most relevantly, this includes counts of 1,000,000 to 50,000,000, differences between bulk and defect lifetimes (τ_2-τ_B) of 0.02 to 0.1 ns, and defect intensities I_2 of 10% to 90%. It should also be emphasized that this formulation assumes perfect knowledge of the IRF. If a negative error is predicted, this indicates that the experimental situation nears or moves outside the range of applicability and that a reasonable decomposition is likely feasible.

III. CONCLUSION

The intrinsic difficulty of decomposing the PALS spectrum into its constituent lifetimes and intensities is demonstrated, and a methodology for determining whether an optimum decomposition into physically significant lifetimes can be obtained is developed. In a range of typical experimental scenarios, the global minimum of the objective function does not represent the true solution. The optimality of different objective functions is considered and it is concluded that the function currently employed in standard fitting methods cannot be improved upon with alternate count weighting schemes. IRF width is shown to have minimal impact on the ability of the objective function to indicate the true solution, but errors are reduced with larger counts. A regression model is developed based on the experimental counts, intensity of the defect lifetime component of the spectrum, and the difference between the defect and bulk lifetime which predicts the anticipated, intrinsic error of the objective function global minimum in estimating the fraction of positrons which annihilate in the bulk. This can be employed to determine whether there is potential to achieve a successful decomposition, or if the average positron lifetime should be reported instead. By using Equation 6, if the predicted error falls below $\sim$10%, then spectral decomposition will be the preferred PALS spectrum analysis method over average lifetime analysis.

ACKNOWLEDGMENTS

The present work has benefited from the financial support of the US Department of Defense SMART Fellowship, as well as financial support from the Air Force Research Laboratory Space Vehicles Directorate.

IV. DATA AVAILABILITY

The data that support the findings of this study are available from the corresponding author upon reasonable request.

Appendix: Experimental parameter accuracy dependence

[1]D. Petschke and T. E. Staab, "A supervised machine learning approach using naive gaussian bayes classification for shape-sensitive detector pulse

Approved for public release; distribution is unlimited. Public Affairs release approval AFRL-2021-0604.

ACCEPTED MANUSCRIPT
Journal of Applied Physics
AIP Publishing
This is the author's peer reviewed, accepted manuscript. However, the online version of record will be different from this version once it has been copyedited and typeset.
PLEASE CITE THIS ARTICLE AS DOI: 10.1063/5.0049304

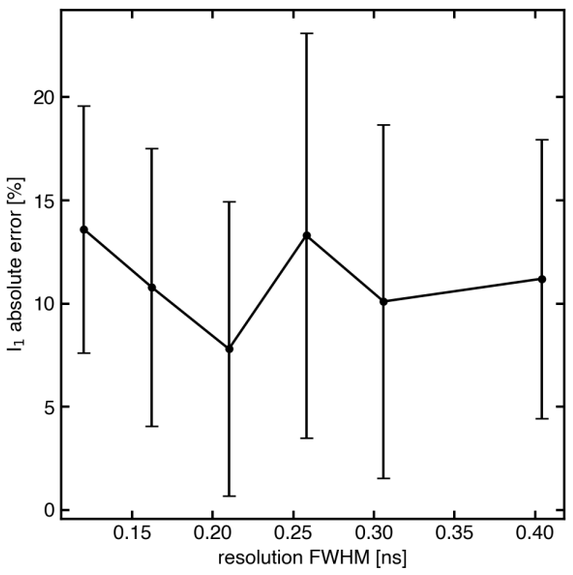

FIG. 8. Error in absolute value of the intensity of the first (bulk) lifetime [%] associated with the objective function global minimum as a function of resolution function FWHM. The error bars show the standard deviation under 10 Poisson samples of the true function. All unspecified spectral parameters are given in Fig. 1 and Table I.

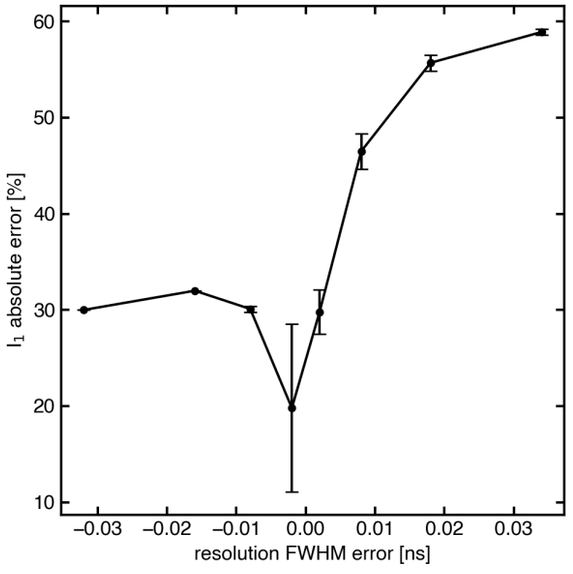

FIG. 9. Error in absolute value of the intensity of the first (bulk) lifetime [%] associated with the objective function global minimum as a function of error in resolution function FWHM error. The error bars show the standard deviation under 10 Poisson samples of the true function. All unspecified spectral parameters are given in Fig. 1 and Table I

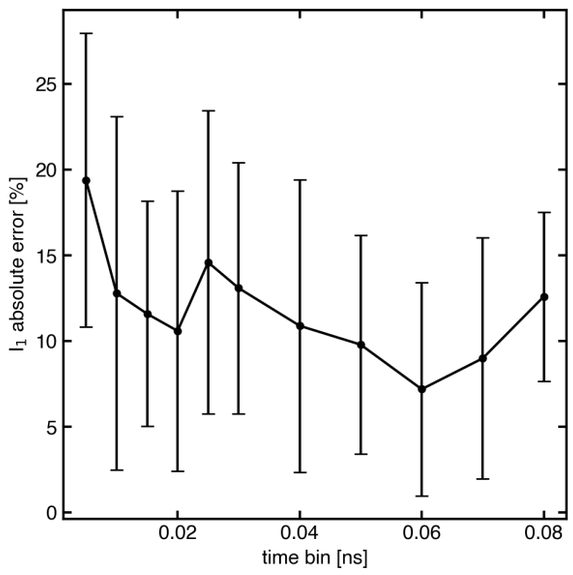

FIG. 10. Error in absolute value of the intensity of the first (bulk) lifetime [%] associated with the objective function global minimum as a function of spectrum time bin width. The error bars show the standard deviation under 10 Poisson samples of the true function. All unspecified spectral parameters are given in Fig. 1 and Table I

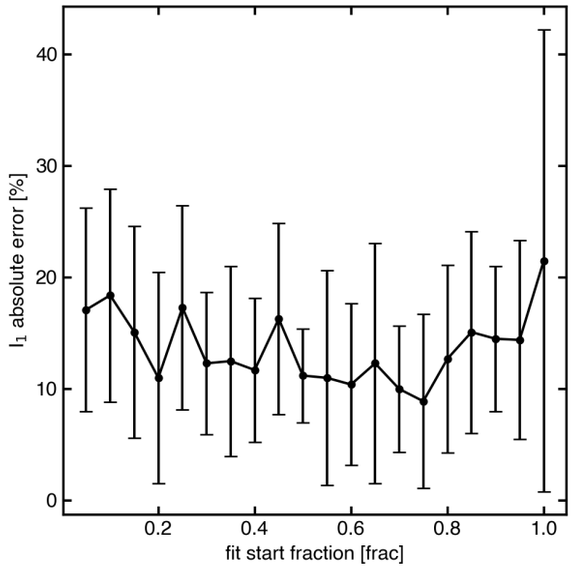

FIG. 11. Error in absolute value of the intensity of the first (bulk) lifetime [%] associated with the objective function global minimum as a function of fit start bin (associated with where counts on the left-hand side of the maximum reach a given percentage of the maximum). The error bars show the standard deviation under 10 Poisson samples of the true function. All unspecified spectral parameters are given in Fig. 1 and Table I

Approved for public release; distribution is unlimited. Public Affairs release approval AFRL-2021-0604.

ACCEPTED MANUSCRIPT
Journal of Applied Physics
AIP Publishing
This is the author's peer reviewed, accepted manuscript. However, the online version of record will be different from this version once it has been copyedited and typeset.
PLEASE CITE THIS ARTICLE AS DOI: 10.1063/5.0049304

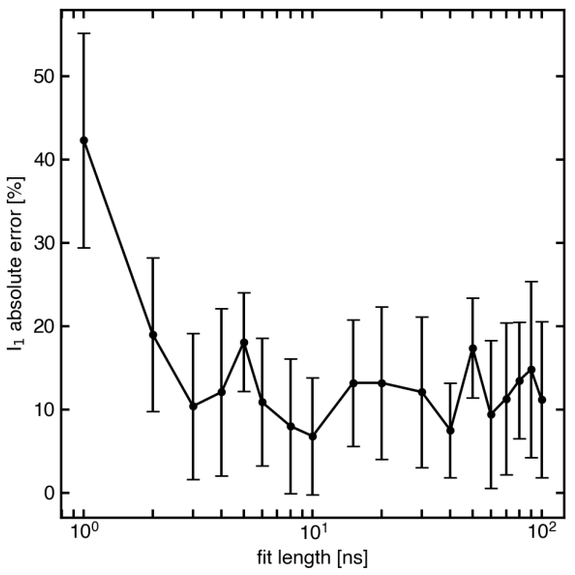

FIG. 12. Error in absolute value of the intensity of the first (bulk) lifetime [%] associated with the objective function global minimum as a function of where in time the fit ends (as quantified by fit length). The error bars show the standard deviation under 10 Poisson samples of the true function. All unspecified spectral parameters are given in Fig. 1 and Table I

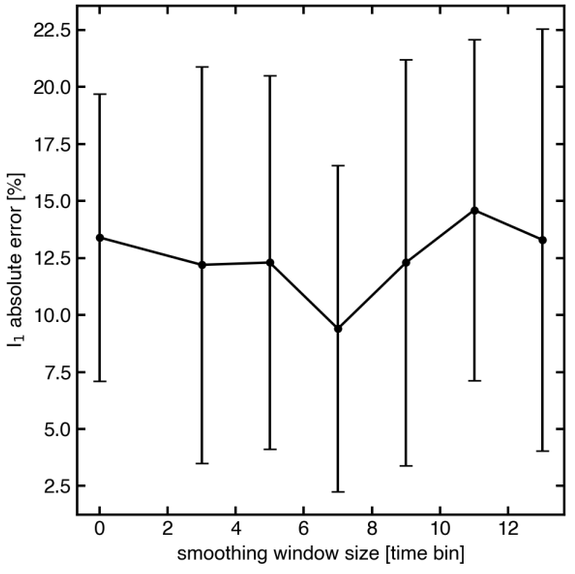

FIG. 13. Error in absolute value of the intensity of the first (bulk) lifetime [%] associated with the objective function global minimum as a function of smoothing window size (Savitzky-Golay filter of order=min(3,window-2)). The error bars show the standard deviation under 10 Poisson samples of the true function. All unspecified spectral parameters are given in Fig. 1 and Table I

discrimination in positron annihilation lifetime spectroscopy (pals)," Nuclear Instruments and Methods in Physics Research Section A: Accelerators, Spectrometers, Detectors and Associated Equipment **947**, 162742 (2019).
[2]R. Krause-Rehberg, R. Leipner, and H. Leipner, *Positron Annihilation in Semiconductors: Defect Studies*, Springer Series in Solid-State Sciences (Springer, 1999).
[3]W. Zhang, B. Gu, J. Liu, and B. Ye, "Accurate theoretical prediction on positron lifetime of bulk materials," Computational Materials Science **105**, 32 – 38 (2015).
[4]Z. quan Chen, Z. Wang, and S. jie Wang, "Interaction between dopants and native defects in Zn doped p-InP observed by positron annihilation," Chinese Physics Letters **16**, 586–588 (1999).
[5]A. Polity, T. Abgarjan, and R. Krause-Rehberg, "Defects in electron irradiated GaP studied by positron lifetime spectroscopy," Applied Physics A Materials Science Processing **60**, 541–544 (1995).
[6]A. Polity, F. Rudolf, C. Nagel, S. Eichler, and R. Krause-Rehberg, "Defects in electron-irradiated GaAs studied by positron lifetime spectroscopy," Phys. Rev. B **55**, 10467–10479 (1997).
[7]W. Arafa and M. Abd El Wahab, "Positron annihilation spectroscopy in the evaluation of microstructure of cast copper and copper-aluminum alloys during isochronal annealing," Journal of materials engineering and performance **14**, 473–479 (2005).
[8]R. M. de la Cruz, R. Pareja, R. González, L. A. Boatner, and Y. Chen, "Effect of thermochemical reduction on the electrical, optical-absorption, and positron-annihilation characteristics of ZnO crystals," Phys. Rev. B **45**, 6581–6586 (1992).
[9]A. Ingram, R. Golovchak, M. Kostrzewa, S. Wacke, M. Shpotyuk, and O. Shpotyuk, "Compositional dependences of average positron lifetime in binary as–s/se glasses," Physica B: Condensed Matter **407**, 652–655 (2012).
[10]S. K. Gupta, C. Reghukumar, N. Pathak, K. Sudarshan, D. Tyagi, M. Mohapatra, P. Pujari, and R. Kadam, "Speciation of uranium and doping induced defects in gd1.98u0.02zr2o7: Photoluminescence, x-ray photoelectron and positron annihilation lifetime spectroscopy," Chemical Physics Letters **669**, 245–250 (2017).
[11]J. Kujala, N. Segercrantz, F. Tuomisto, and J. Slotte, "Native point defects in gasb," Journal of Applied Physics **116**, 143508 (2014), https://doi.org/10.1063/1.4898082.
[12]P. Kirkegaard, J. V. Olsen, and M. M. Eldrup, *PALSfit3: A software package for analysing positron lifetime spectra* (Technical University of Denmark, 2017).
[13]P. J. Foster, P. Mascher, A. P. Knights, and P. G. Coleman, "Implantation profile of Na22 continuous energy spectrum positrons in silicon," Journal of Applied Physics **101**, 043702 (2007), https://doi.org/10.1063/1.2472645.
[14]A. Zubiaga, F. Plazaola, J. A. García, F. Tuomisto, V. Muñoz Sanjosé, and R. Tena-Zaera, "Positron annihilation lifetime spectroscopy of ZnO bulk samples," Phys. Rev. B **76**, 085202 (2007).
[15]V. Avalos and S. Dannefaer, "Positron-annihilation investigation of vacancy agglomeration in electron-irradiated float-zone silicon," Phys. Rev. B **54**, 1724–1728 (1996).
[16]F. Tuomisto, "Point defects and impurities in bulk GaN studied by positron annihilation spectroscopy," in *Technology of Gallium Nitride Crystal Growth*, edited by D. Ehrentraut, E. Meissner, and M. Bockowski (Springer Berlin Heidelberg, Berlin, Heidelberg, 2010) pp. 295–316.
[17]C. Corbel, M. Stucky, P. Hautojärvi, K. Saarinen, and P. Moser, "Positron-annihilation spectroscopy of native vacancies in as-grown GaAs," Phys. Rev. B **38**, 8192–8208 (1988).
[18]J. Gebauer, F. Börner, R. Krause-Rehberg, T. E. M. Staab, W. Bauer-Kugelmann, G. Kögel, W. Triftshäuser, P. Specht, R. C. Lutz, E. R. Weber, and M. Luysberg, "Defect identification in GaAs grown at low temperatures by positron annihilation," Journal of Applied Physics **87**, 8368–8379 (2000), https://doi.org/10.1063/1.373549.
[19]P. Horodek, K. Siemek, J. Dryzek, and M. Wróbel, "Positron annihilation and complementary studies of copper sandblasted with alumina particles at different pressures," Materials **10**, 1343 (2017).
[20]D. T. Britton, P. Willutzki, T. E. Jackman, and P. Mascher, "Positron lifetime studies of defects in MBE-grown silicon," Journal of Physics: Condensed Matter **4**, 8511–8518 (1992).
[21]A. Zubiaga, F. Plazaola, J. A. García, F. Tuomisto, V. Muñoz Sanjosé, and R. Tena-Zaera, "Positron annihilation lifetime spectroscopy of zno bulk

Approved for public release; distribution is unlimited. Public Affairs release approval AFRL-2021-0604.

ACCEPTED MANUSCRIPT
Journal of Applied Physics
AIP Publishing
This is the author's peer reviewed, accepted manuscript. However, the online version of record will be different from this version once it has been copyedited and typeset.
PLEASE CITE THIS ARTICLE AS DOI: 10.1063/5.0049304

samples," Phys. Rev. B **76**, 085202 (2007).
[22]G. Brauer, W. Anwand, W. Skorupa, J. Kuriplach, O. Melikhova, C. Moisson, H. von Wenckstern, H. Schmidt, M. Lorenz, and M. Grundmann, "Defects in virgin and n^+-implanted zno single crystals studied by positron annihilation, hall effect, and deep-level transient spectroscopy," Phys. Rev. B **74**, 045208 (2006).
[23]B. Somieski, T. Staab, and R. Krause-Rehberg, "The data treatment influence on the spectra decomposition in positron lifetime spectroscopy part 1: On the interpretation of multi-component analysis studied by monte carlo simulated model spectra," Nuclear Instruments and Methods in Physics Research Section A: Accelerators, Spectrometers, Detectors and Associated Equipment **381**, 128 – 140 (1996).

Approved for public release; distribution is unlimited. Public Affairs release approval AFRL-2021-0604.

AIP Publishing

Journal of Applied Physics

ACCEPTED MANUSCRIPT

This is the author's peer reviewed, accepted manuscript. However, the online version of record will be different from this version once it has been copyedited and typeset.
PLEASE CITE THIS ARTICLE AS DOI: 10.1063/5.0049304

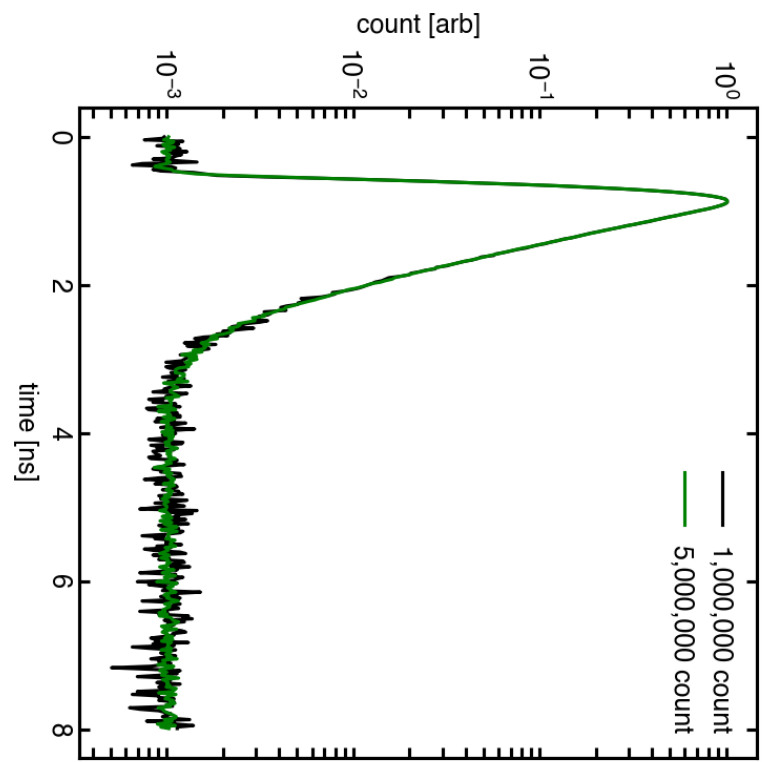

ACCEPTED MANUSCRIPT

Journal of Applied Physics

This is the author's peer reviewed, accepted manuscript. However, the online version of record will be different from this version once it has been copyedited and typeset.
PLEASE CITE THIS ARTICLE AS DOI: 10.1063/5.0049304

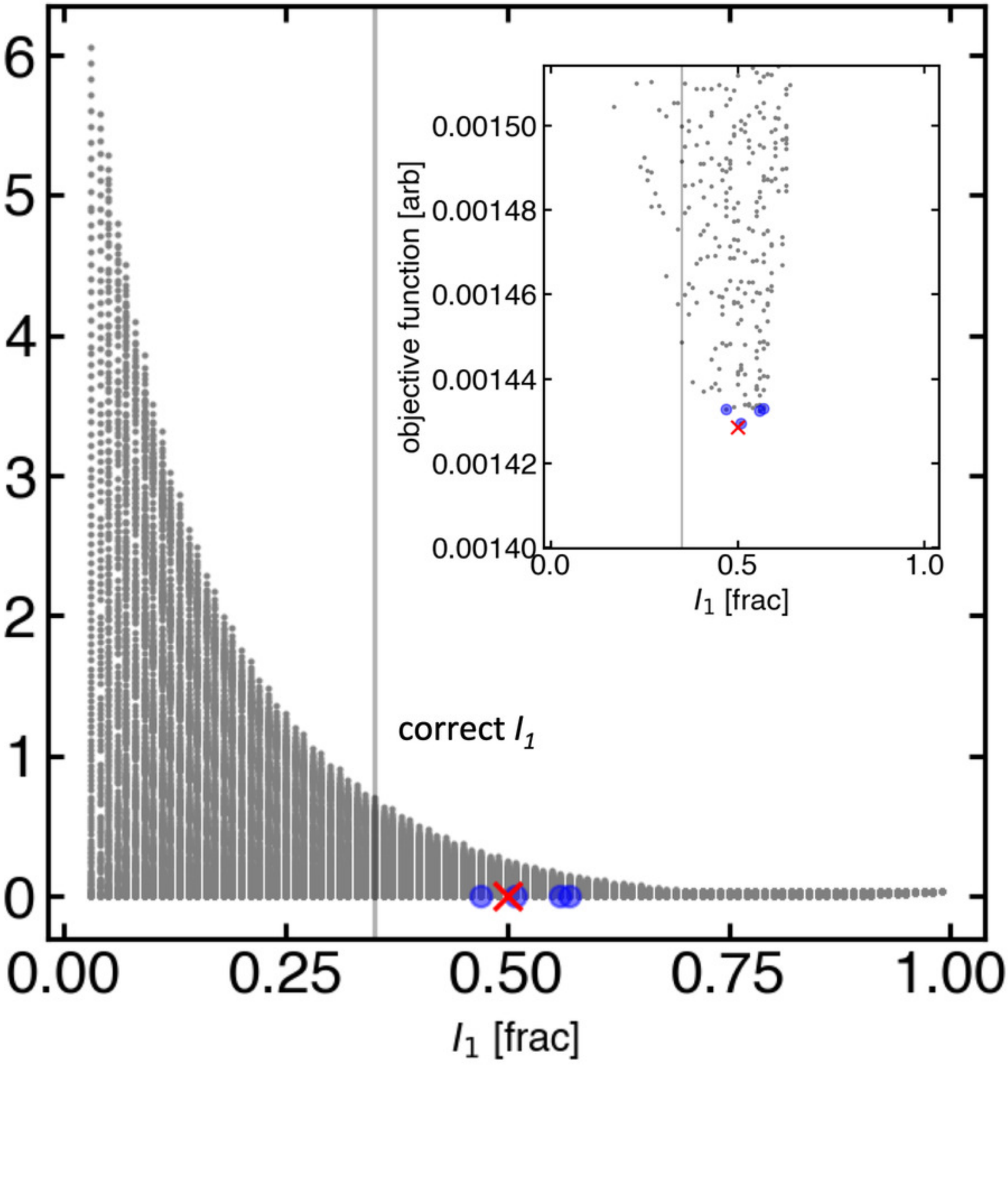

AIP Publishing

Journal of Applied Physics

ACCEPTED MANUSCRIPT

This is the author's peer reviewed, accepted manuscript. However, the online version of record will be different from this version once it has been copyedited and typeset.
PLEASE CITE THIS ARTICLE AS DOI: 10.1063/5.0049304

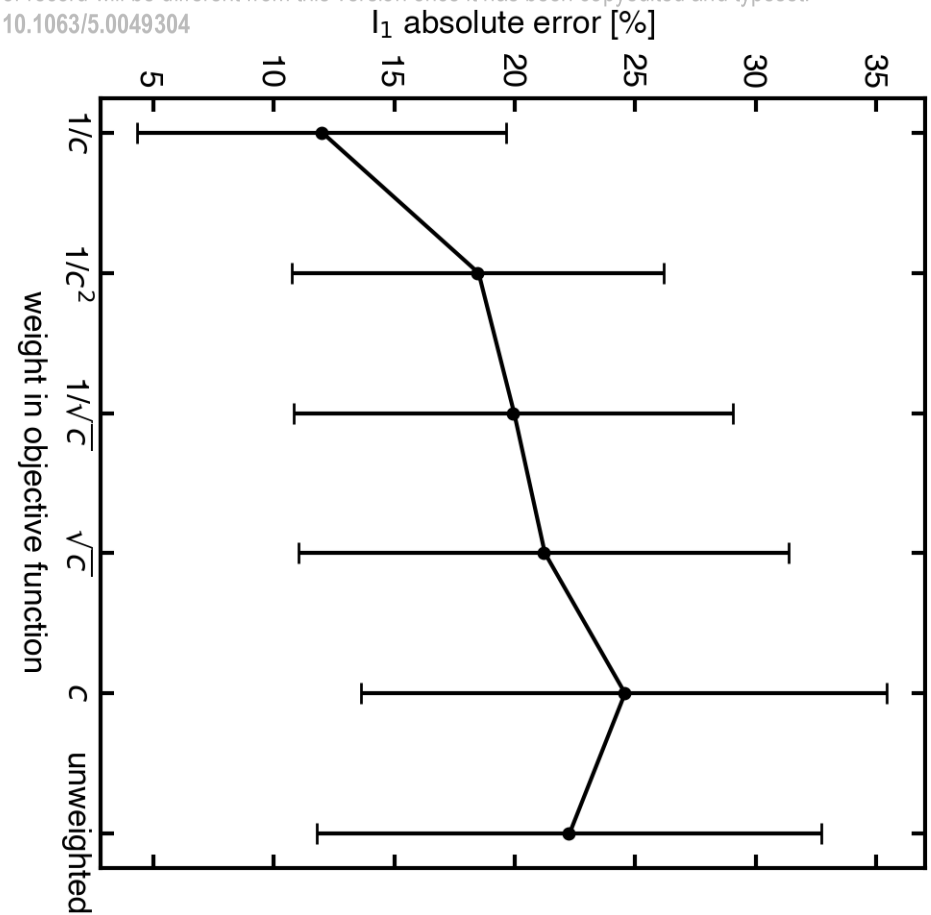

ACCEPTED MANUSCRIPT
Journal of Applied Physics
AIP Publishing
This is the author's peer reviewed, accepted manuscript. However, the online version of record will be different from this version once it has been copyedited and typeset.
PLEASE CITE THIS ARTICLE AS DOI: 10.1063/5.0049304

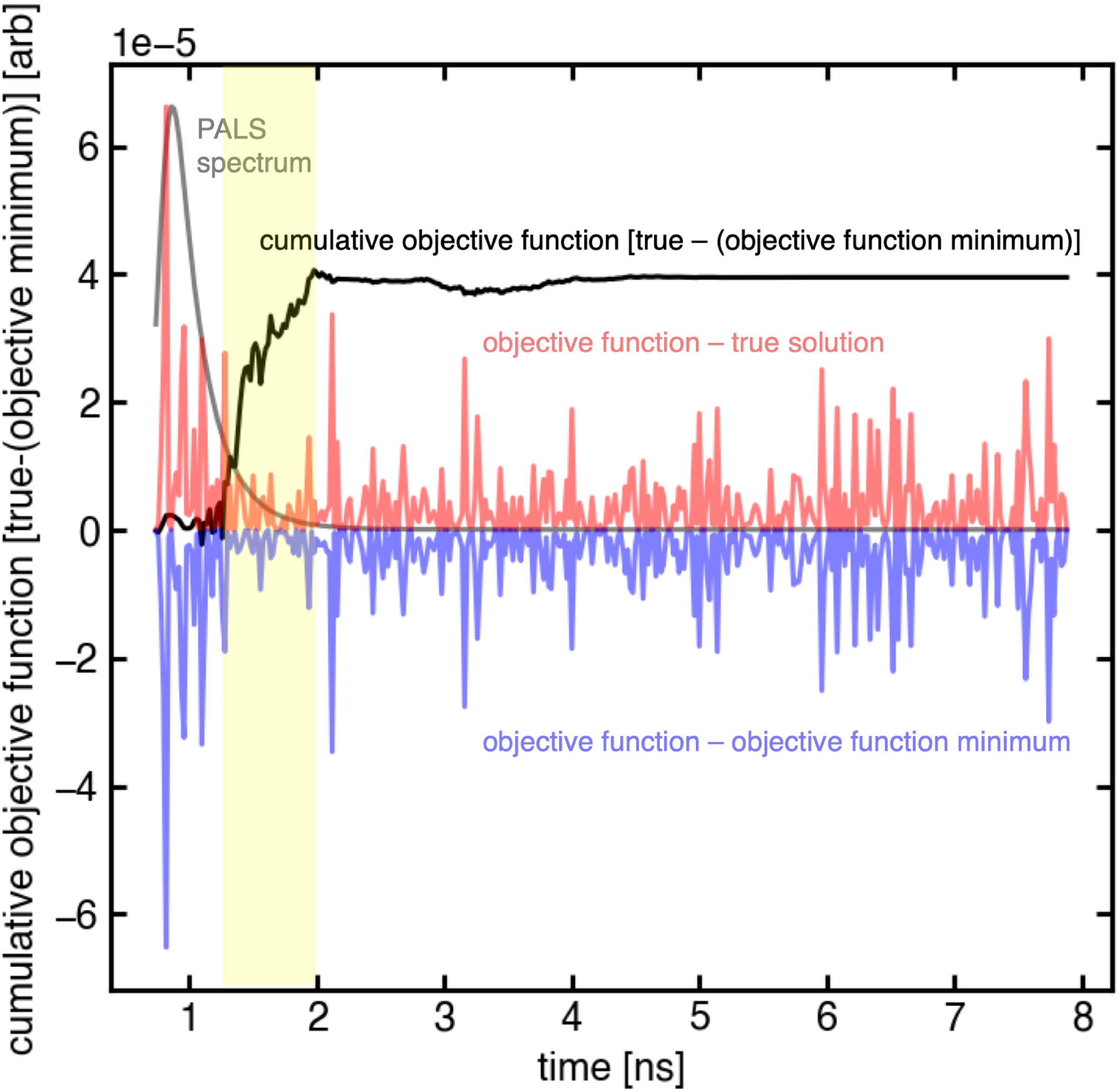

AIP Publishing

Journal of Applied Physics

ACCEPTED MANUSCRIPT

This is the author's peer reviewed, accepted manuscript. However, the online version of record will be different from this version once it has been copyedited and typeset.

PLEASE CITE THIS ARTICLE AS DOI: 10.1063/5.0049304

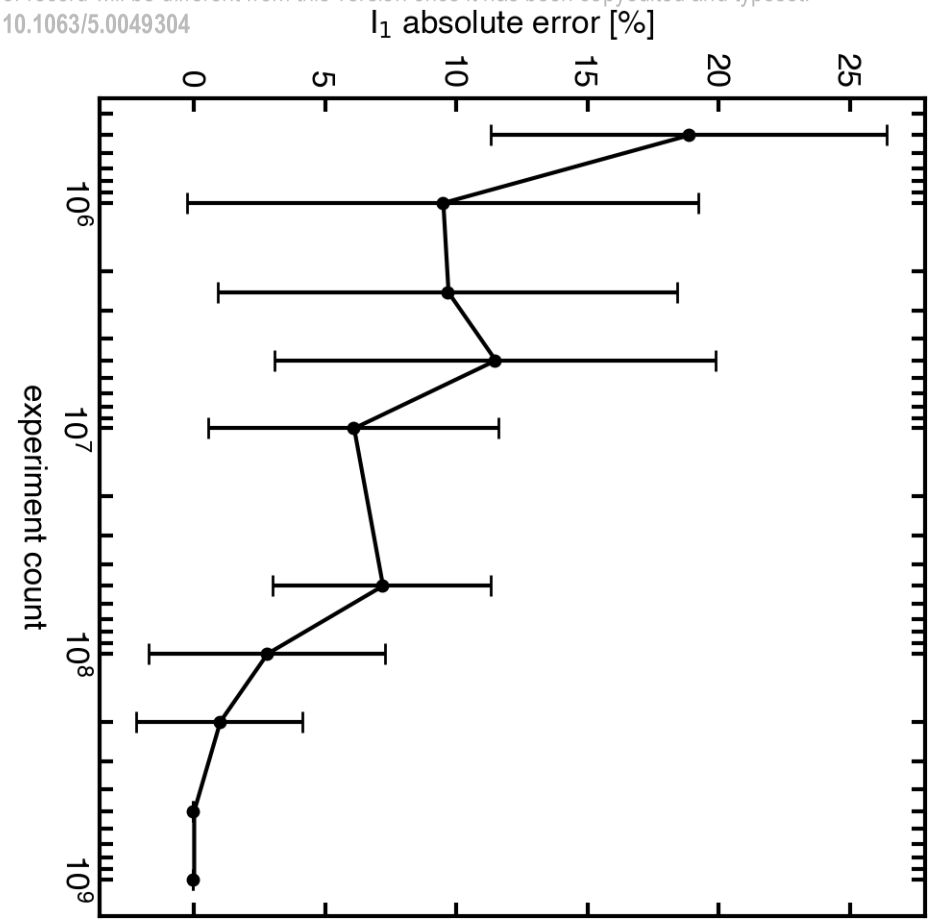

ACCEPTED MANUSCRIPT
Journal of Applied Physics
AIP Publishing
This is the author's peer reviewed, accepted manuscript. However, the online version of record will be different from this version once it has been copyedited and typeset.
PLEASE CITE THIS ARTICLE AS DOI: 10.1063/5.0049304

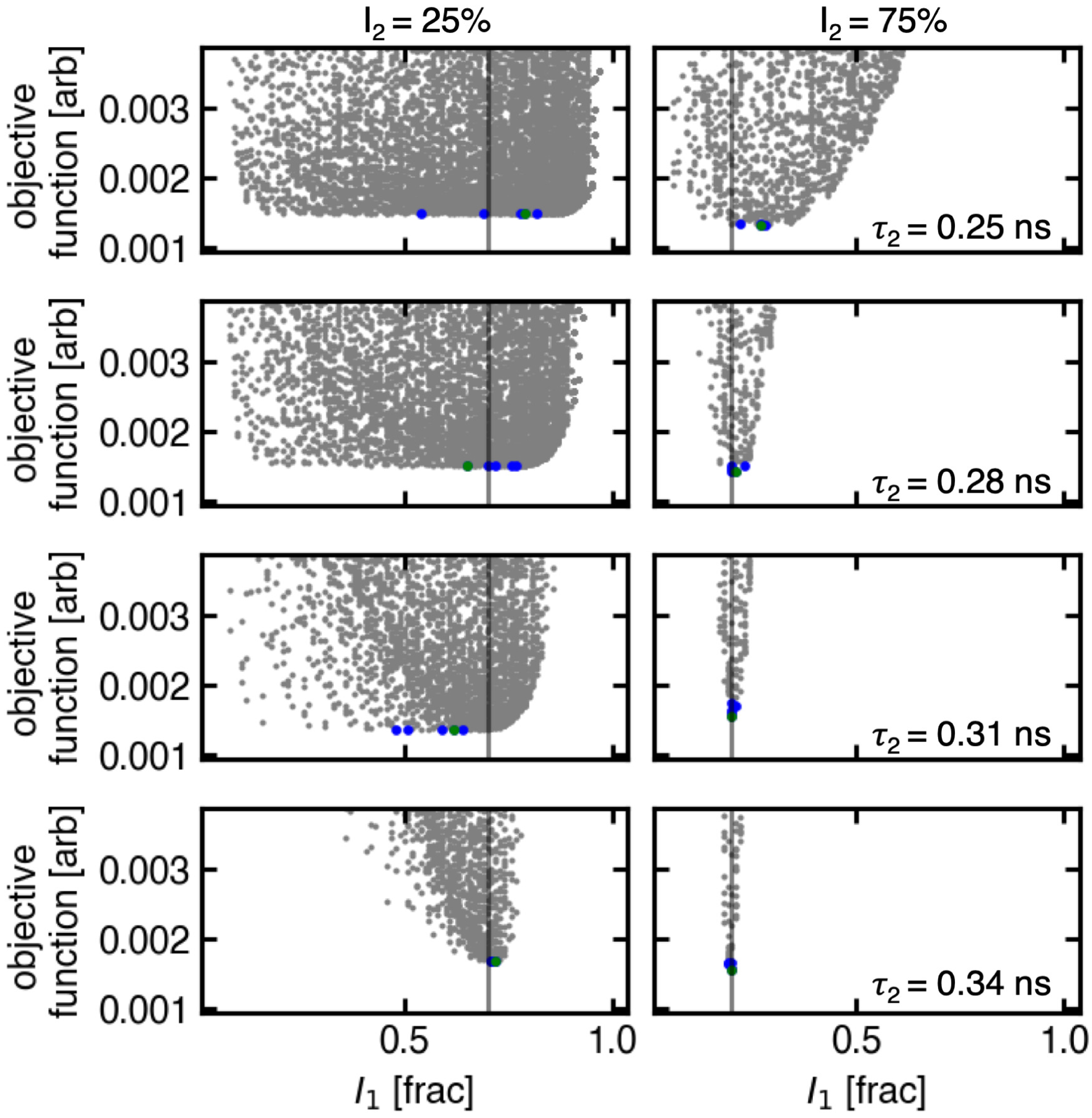

AIP Publishing

Journal of Applied Physics

ACCEPTED MANUSCRIPT

This is the author's peer reviewed, accepted manuscript. However, the online version of record will be different from this version once it has been copyedited and typeset.

PLEASE CITE THIS ARTICLE AS DOI: 10.1063/5.0049304

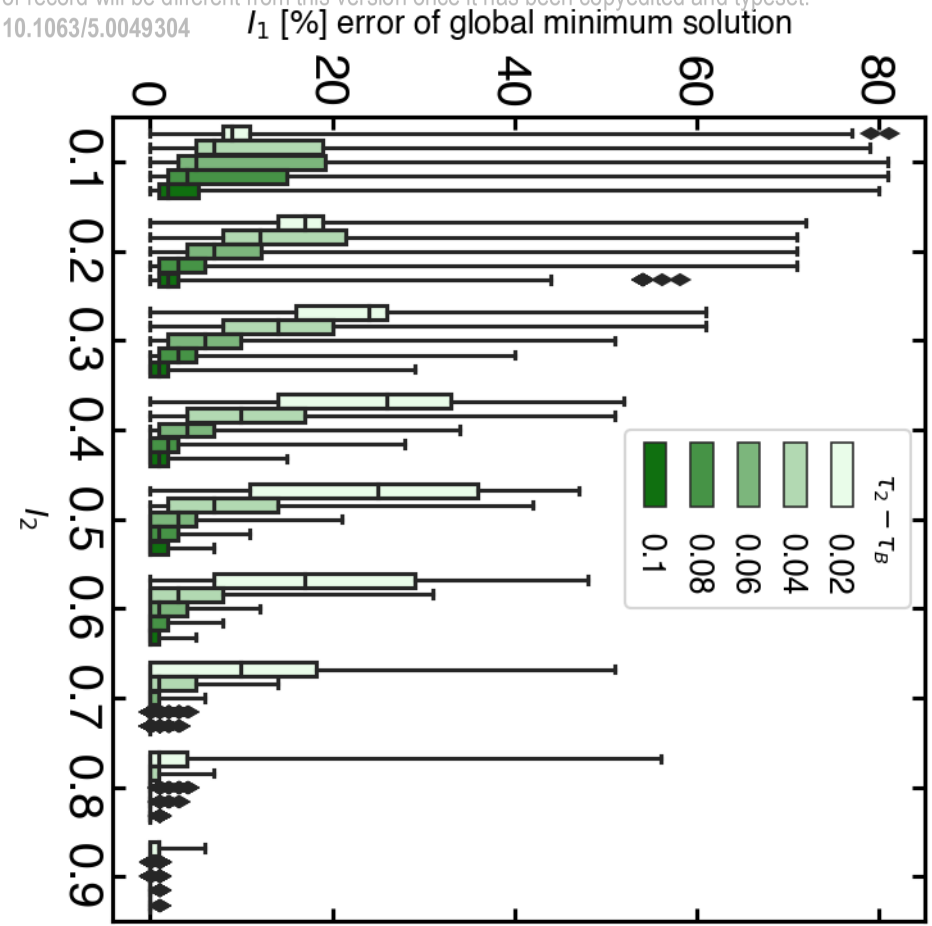

AIP Publishing

Journal of Applied Physics

ACCEPTED MANUSCRIPT

This is the author's peer reviewed, accepted manuscript. However, the online version of record will be different from this version once it has been copyedited and typeset.

PLEASE CITE THIS ARTICLE AS DOI: 10.1063/5.0049304

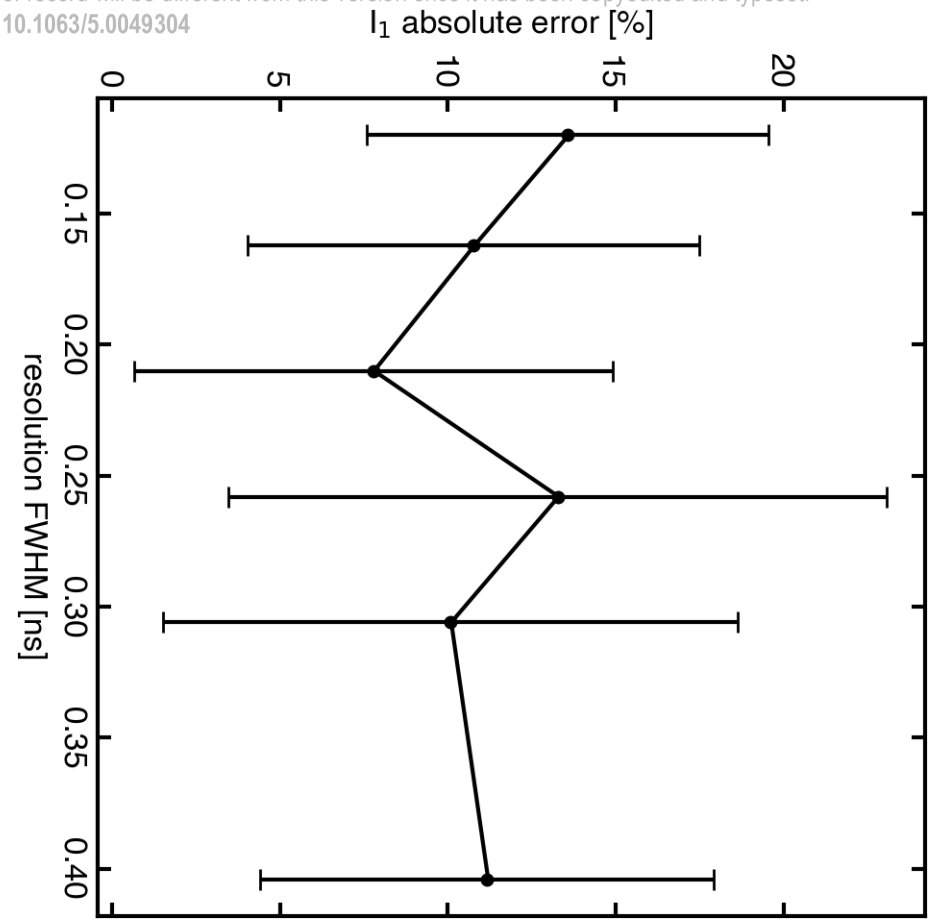

AIP Publishing

Journal of Applied Physics

ACCEPTED MANUSCRIPT

This is the author's peer reviewed, accepted manuscript. However, the online version of record will be different from this version once it has been copyedited and typeset.

PLEASE CITE THIS ARTICLE AS DOI: 10.1063/5.0049304

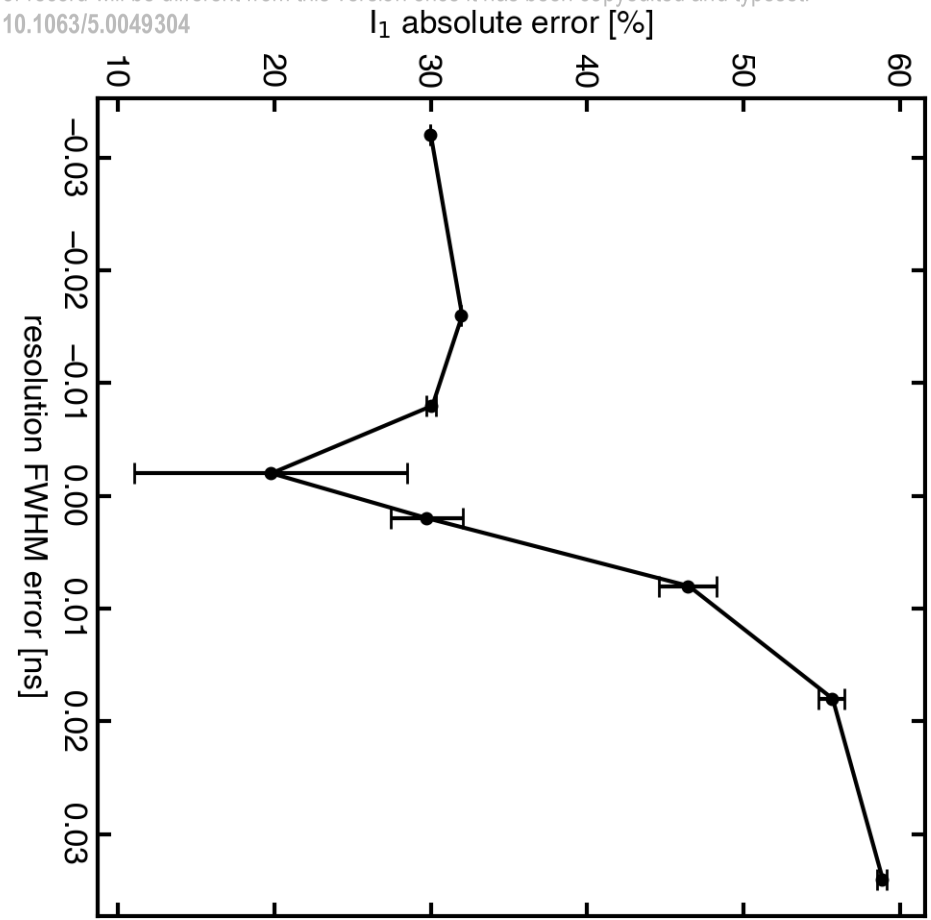

AIP Publishing

Journal of Applied Physics

ACCEPTED MANUSCRIPT

This is the author's peer reviewed, accepted manuscript. However, the online version of record will be different from this version once it has been copyedited and typeset.

PLEASE CITE THIS ARTICLE AS DOI: 10.1063/5.0049304

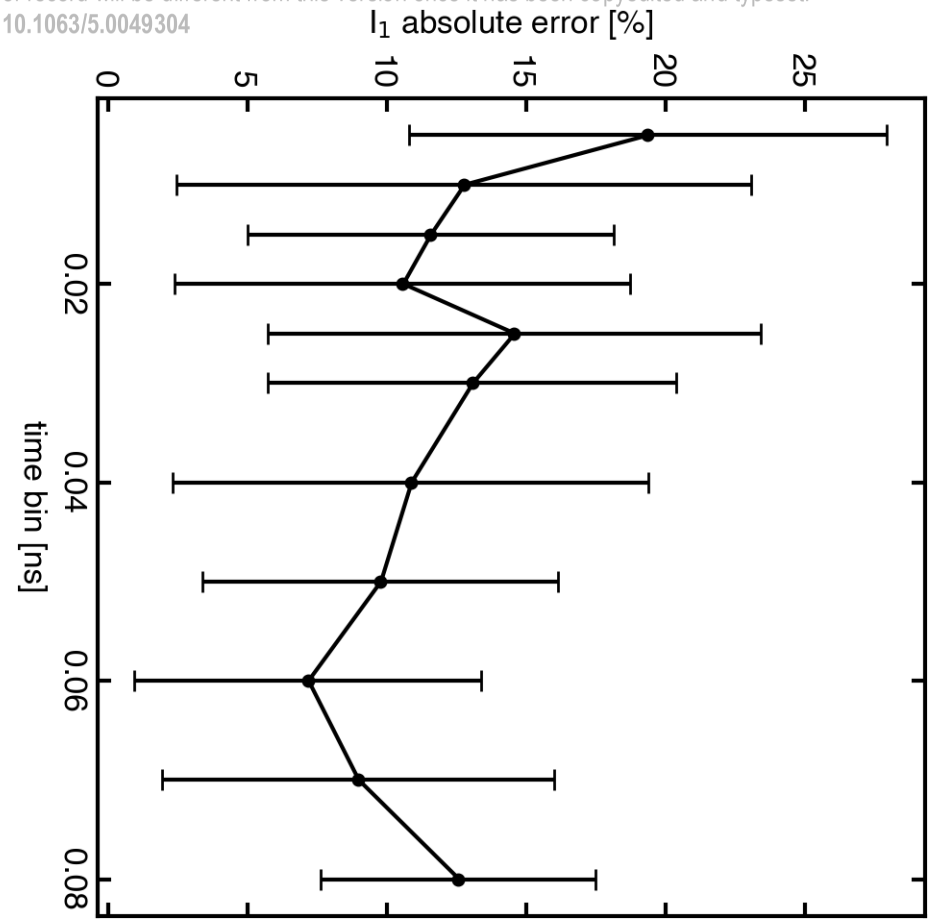

AIP Publishing

Journal of Applied Physics

ACCEPTED MANUSCRIPT

This is the author's peer reviewed, accepted manuscript. However, the online version of record will be different from this version once it has been copyedited and typeset.

PLEASE CITE THIS ARTICLE AS DOI: 10.1063/5.0049304

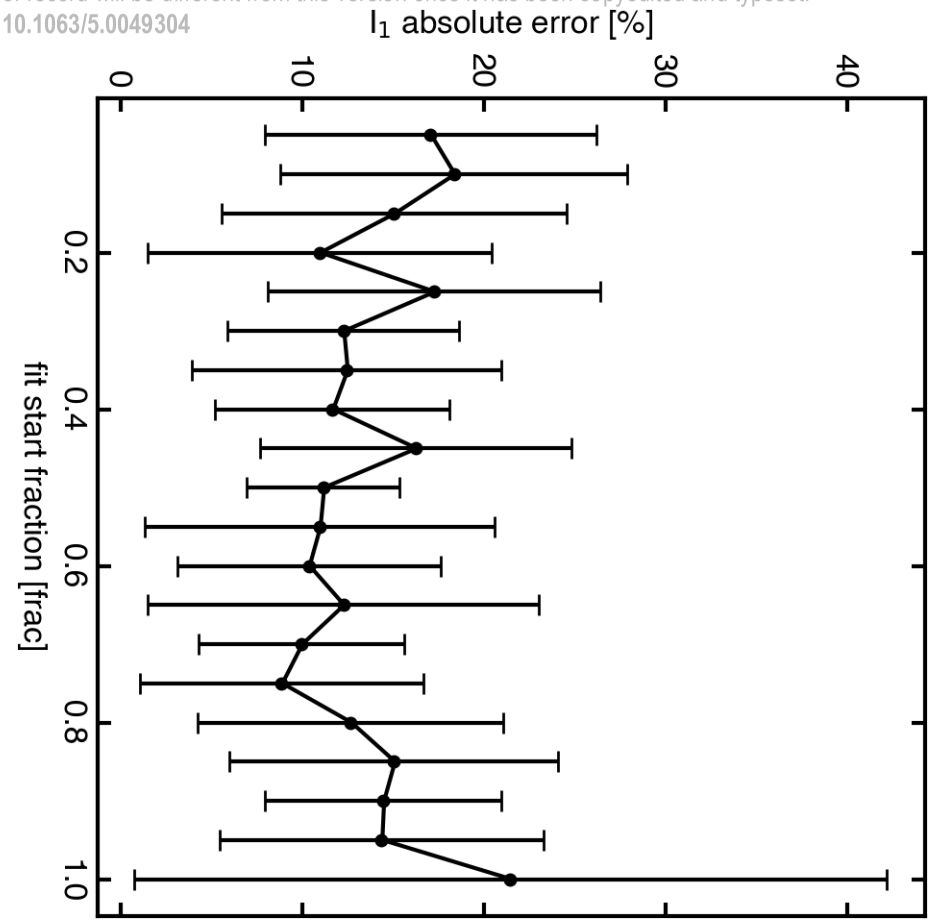

AIP Publishing

Journal of Applied Physics

ACCEPTED MANUSCRIPT

This is the author's peer reviewed, accepted manuscript. However, the online version of record will be different from this version once it has been copyedited and typeset.

PLEASE CITE THIS ARTICLE AS DOI: 10.1063/5.0049304

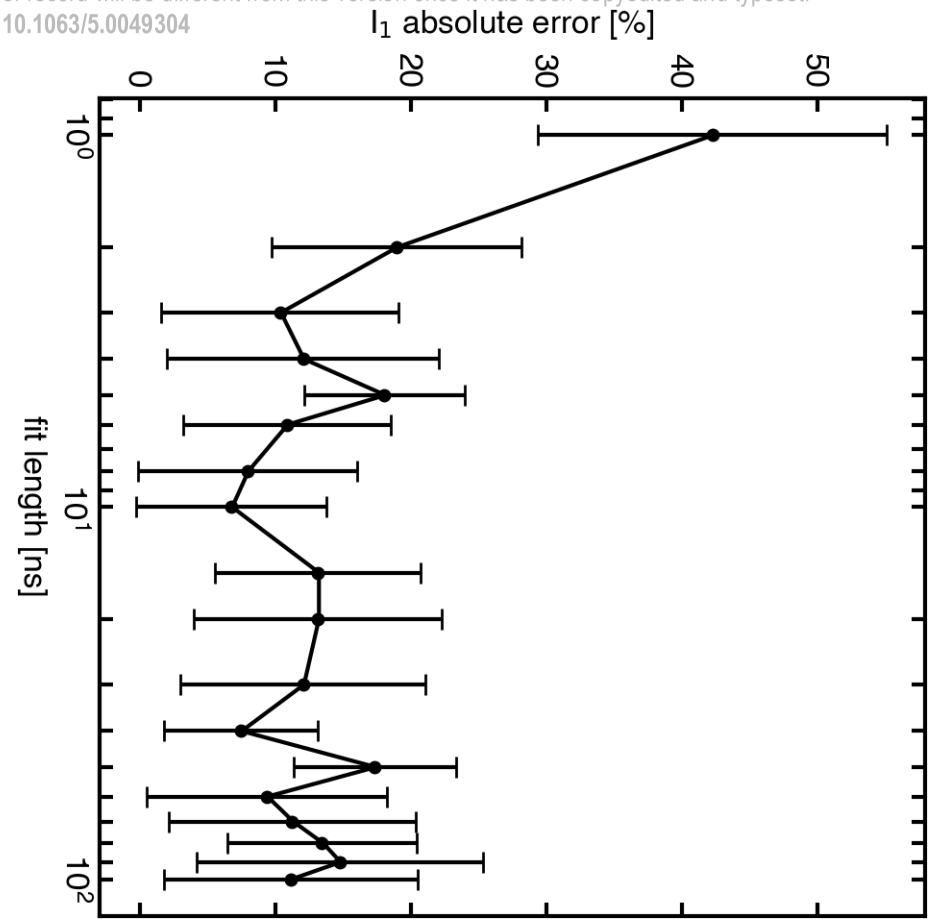

View publication stats

AIP Publishing

Journal of Applied Physics

ACCEPTED MANUSCRIPT

This is the author's peer reviewed, accepted manuscript. However, the online version of record will be different from this version once it has been copyedited and typeset.

PLEASE CITE THIS ARTICLE AS DOI: 10.1063/5.0049304